JOURNAL OF MATERIALS SCIENCE 30 (1995) 1772–1780

# Influence of water on crack propagation in poly methyl methacrylate: craze stress and craze fibril lifetime

L. JOSSERAND, R. SCHIRRER
*Institut Charles Sadron (CRM-EAHP), 4 rue Boussingault, F-67000 Strasbourg, France*
P. DAVIES
*Institut Français pour la Recherche et l'Exploitation de la Mer (IFREMER), F-29280 Plouzane, France*

Polymethylmethacrylate (PMMA) is often used as a material in submarine applications. Therefore, the fracture properties of dry and wet PMMA in water and/or under hydrostatic pressure are of great importance. Previous work has shown that water strongly increases fracture toughness, and leads to a complicated figure of $K_1$ versus crack speed, and stable–unstable crack and craze propagation, depending on external loading rate. In this study, compact tension specimens immersed in water have been tested on a tensile machine and crack tips have been observed during propagation by means of optical interferometry. Fracture stress intensity factors, and craze-zone shapes and sizes have been measured as a function of loading time and crack speed in water. The results have been rationalized in terms of craze fibril stress versus fibril extraction velocity and craze fibril lifetime versus fibril stress. Both may be expressed in terms of a stress-activated process governing fracture. It is found that, when expressed in these terms, the complicated influence of the external loading rate becomes irrelevant for describing local intrinsic material properties and $K_1$ values. It is shown that there is no contradiction between the fact that water increases the fracture toughness, and the fact that the microscopic craze stress and craze fibril lifetime decrease at the crack tip.

## 1. Introduction

Crazing and fracture properties of polymers are strongly influenced by the environment: stress cracking and crazing due to chemical effects, crack-tip plasticizing by liquids or solvent gases, lowering of surface energy by tensio-active liquids, molecular mobility modification by hydrostatic liquid pressure, etc. Environmental fracture has been widely studied, particularly from the experimental point of view, and general rules are known concerning chemical and physical effects of gases and liquids on polymer fracture. Nevertheless, most of these studies use very simple fracture tests to quantify the environmental effects, and, although rather coarse values of environment-affected fracture toughness are known, real-time microscopic crack-tip behaviour under harsh environmental conditions has been much less studied. This is because special experimental equipment is required to investigate the material in this case. The very abundant literature on environment-assisted crazing and fracture of polymers will not be reviewed here, and attention will be focussed on the effect of water on fracture toughness.

From the linear elastic fracture mechanics point of view, water acts in the following way on a propagating crack tip in PMMA. It was determined very early [1] that specific work for fracture in PMMA in water is about four times higher than in air with unstable propagation, and that the loading rate and crack speed are important parameters [2]. It is also known that water acts like a mild crazing agent, lowering crazing stress, and leading to faster craze growth [3]. Unstable crack propagation has been carefully examined in water [4], and it has been shown that Williams' model [5] does not describe the observed behaviour. On the other hand, when breaking in air un-notched samples cut from PMMA which was previously saturated with water, it appears that the brittleness increases at high water content [6], due to the appearance of water clusters in the material.

From the small-strain mechanical behaviour point of view, PMMA containing water shows a small increase in internal friction at low temperature ( − 100 to − 150 °C) [6, 7], 50% of the water being taken up by swelling and the remaining 50% being accommodated in microvoids [8, 9]. Experiments on stretched PMMA showed that the water sorption depends on


0022–2461 

the molecular orientation, and relaxation experiments show that the glass transition temperature decreases by about 25 °C [10], cross-linking also being an important parameter [11]. Creep behaviour of water-saturated PMMA has also been investigated, using time–temperature shift factors [12]. Finally, cyclic loading lifetime has been shown to be reduced by a factor of up to 500 when PMMA is water saturated [13].

In the present study, it was confirmed that water decreases the small-strain mechanical properties of PMMA by means of a plasticizing mechanism, but the changes were rather small. The single craze at a crack tip propagating in PMMA in air and water has been investigated on a microscopic scale. Local material properties such as craze fibril stress and craze fibril lifetime have been investigated by means of optical interferometry. These fracture properties are much more strongly affected than the small-strain mechanical properties.

The material used was a commercial grade of the Altuglas PMMA from Altulor company (cast sheets). The sheets were 4, 2.5 and 1.5 mm thick. The advantage of this material is that there are already a large number of general mechanical property measurements available from many authors.

## 2. Influence of water on general properties

### 2.1. Diffusion kinetics

The water diffusion coefficient in PMMA is rather low, and the time to saturate sheets is extremely long. Fig. 1 shows the water absorption of PMMA immersed in distilled water at 20 °C. A 1.5 mm thick sheet takes about 2 months to be fully saturated. The diffusion is governed by the well-known Fick's law. The diffusion coefficient measured on Fig. 1 is $1.7 \times 10^7 \text{mm}^2 \text{s}^{-1}$ at 20 °C. The saturated water content is about 1.9%, and seems to vary only slightly with temperature. Conversely, the diffusion coefficient is strongly affected by temperature. Samples have been saturated at 5, 20, 40, 60 and 80 °C. The diffusion coefficient follows an Arrhenius law, with an activation energy of 27 kJ $\text{mol}^{-1}$, which is a normal experimental value. The same experiment was performed at 20 °C under $6 \times 10^7$ Pa (600 bar) to simulate deep-sea pressure. The diffusion coefficient remained at that temperature, the same as that determined without pressure.

### 2.2. Size effect

At the crack tip, the crazed zone has an extremely high surface-to-volume ratio. Therefore, the time to saturate the craze fibrils with water may be much shorter than that reported for the bulk material. The Fickian equation allows such a calculation. Nevertheless, the result obtained must be considered as an order of magnitude estimation rather than a precise value: the PMMA in the craze fibrils is highly stretched (200%–500% deformation, more than 50 MPa local stress), the space between the fibrils is very narrow (10–100 nm). This may result in different diffusion phenomena, connected with surface-tension effects between water and PMMA.

Fig. 2 shows the calculated depth of the Fickian water front at 50%, 75% and 95% (relative to saturation) water content, as a function of time. The equation uses the "erfc" function, solution from the diffusion equation

$$C(x,t)/C_0 = \text{erfc}[D,t,x/2] \quad (1)$$

where $x$, $t$ and $D$ are depth, time and diffusion coefficient, respectively. $C_0$ is the saturated water content, and $C(x,t)$ the kinetic water content at the depth $x$. This figure shows that a 100 nm, craze fibril is saturated in 1 s. Therefore, one can assume that there will exist at least two craze fibril growth mechanisms,

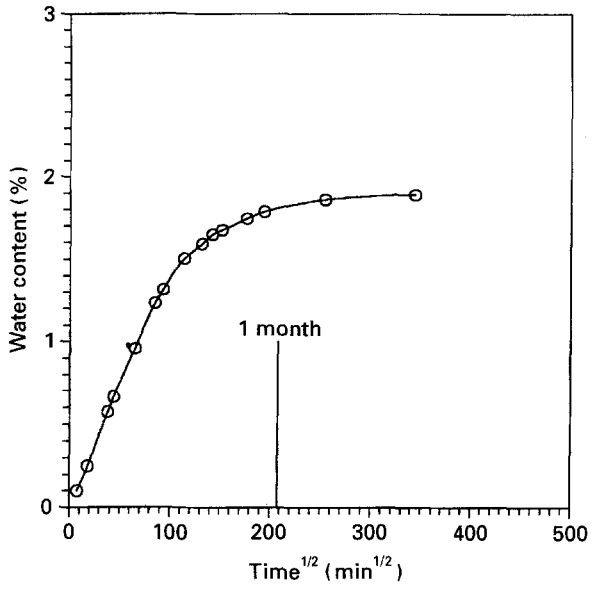


*Figure 1* Water content versus square root of time, for a $1.5 \times 40 \times 40$ mm$^3$ sample at 20 °C.

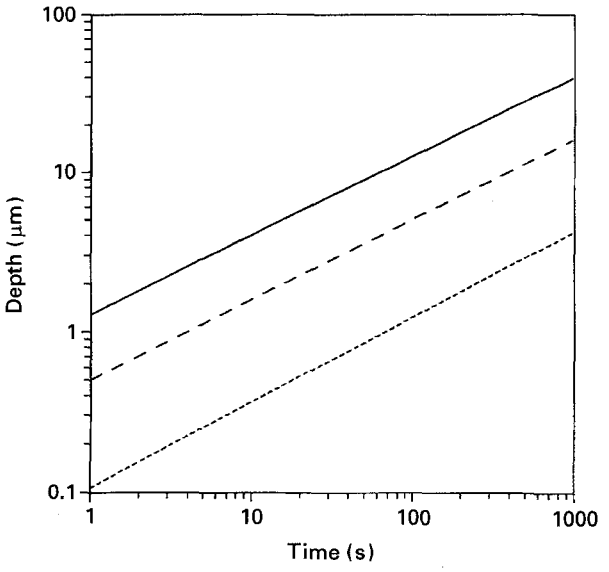


*Figure 2* Size effects: water-front position. Relative water content: (---) 95%, (– –) 75%, (——) 50%. Diffusion coefficient $1.7 \times 10^6 \text{mm}^2 \text{s}^{-1}$ at 20 °C.

depending on whether the time the fibrils are subjected to water is shorter or longer than some characteristic exposure time.

## 2.3. Influence of water on glass transition temperature, $T_g$

It is generally accepted that absorbed water acts like a plasticizer in polymers. This leads to a lowering of the glass transition temperature. The swelling of PMMA as a function of water content has shown that the density of the water containing PMMA remains almost unchanged. Probably some of the water molecules fill the so-called "free volume", and the others swell the material. The latter are probably chemically linked to PMMA molecules, and reduce the chain friction, decreasing the glass transition temperature. The glass transition temperature, $T_g$, measured by means of DSC (differential scanning calorimetry), is given in Table I. The first scan shows that $T_g$ decreases a little with water content. The decrease in $T_g$ between the first and second scan for 0 and 0.7 wt % water content is known and due to molecular rearrangements. For 1.9 wt % water content, $T_g$ increases between the first and the second scan, as part of the water (trapped in the "free volume") is likely to evaporate quickly. It should be mentioned that the DSC curves do not show a peak at 100 °C.

## 2.4. Influence on modulus and yield stress

Tensile tests have been performed on 1.5 mm thick PMMA samples containing 0, 0.8, 1.2 and 1.8 wt % water. The samples were immersed in water until their weight increased to the chosen percentage, and subsequently they were sealed in bags for 21 days to allow the homogeneous diffusion of the water through the sample thickness.

The results are shown in Fig. 3. The tensile modulus decreases by about 10%, and the yield stress 20% for 1.8 wt % water content. The yield stress (defined as the stress, $\sigma$, at which $\delta\sigma/\delta\varepsilon = 0$) was difficult to obtain for dry samples which break too early. The values were obtained by extrapolating the stress–strain curve.

## 2.5. Conclusion

Water decreases the small-strain mechanical properties of PMMA by means of plasticizing mechanisms, but the changes are rather small. As shown below, the fracture properties are much more strongly affected than the small-strain mechanical properties.

TABLE I The glass transition temperature, $T_g$, measured by means of DSC.

| | Water content (wt %) | | |
|---|---|---|---|
| | 0 | 0.7 | 1.9 |
| $T_g$ first scan | 118.9 | 111.2 | 104.3 |
| | | | 103.7 |
| (°C) | | | 103.8 |
| $T_g$ second scan | 115.6 | 107.4 | 107.4 |
| same sample (°C) | | | 107.4 |

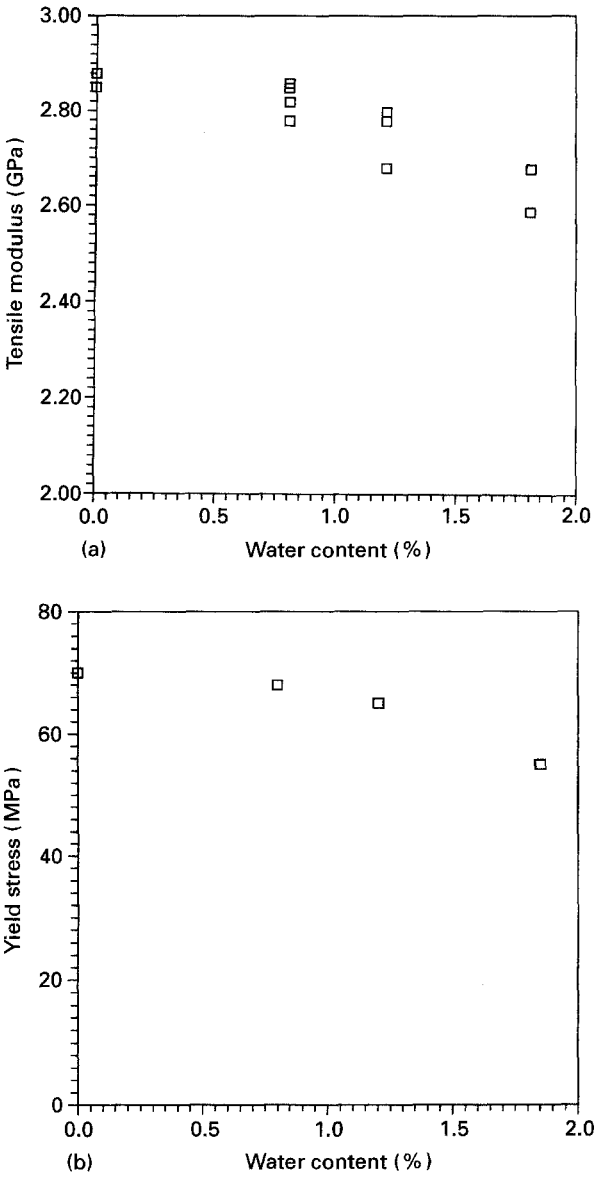


*Figure 3* (a) Tensile modulus versus water content. (b) Yield stress versus water content.

## 3. Fracture properties in water

All the results presented below concern crack and/or craze propagation in dry PMMA immersed in water during the propagation. This is the most realistic case in practical use, due to the very low water diffusion coefficient combined with the fact that the PMMA components employed in marine applications are mainly in air and only occasionally immersed. Therefore, the water diffusion kinetics concern mainly the very narrow crack-tip zone.

## 3.1. Tensile tests

Fracture toughness was measured on 30 mm wide standard compact tension specimens. The crack and craze velocity were obtained with a telescope fitted on to a camera. The sample was illuminated with white

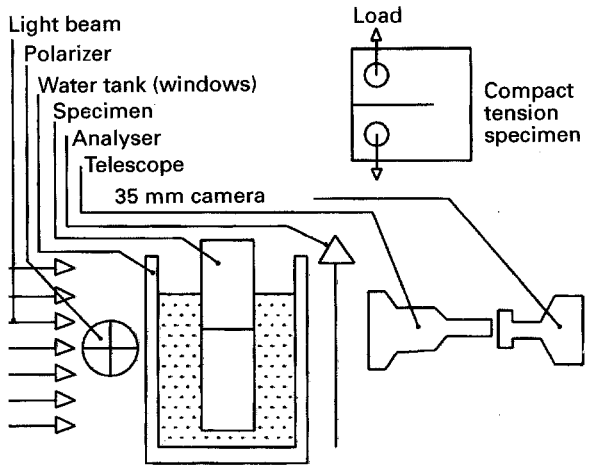


*Figure 4* Tensile machine apparatus.

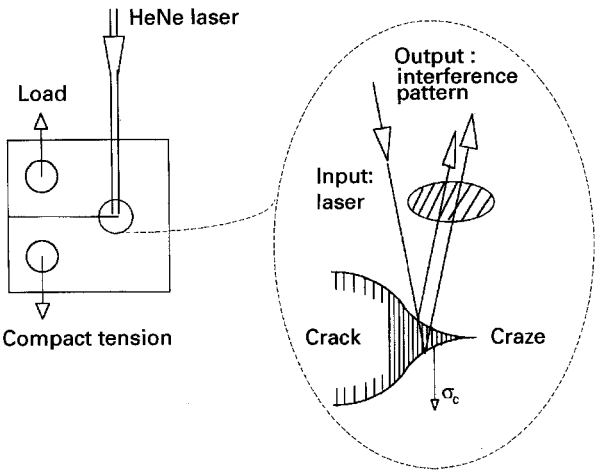


*Figure 6* Experimental apparatus.

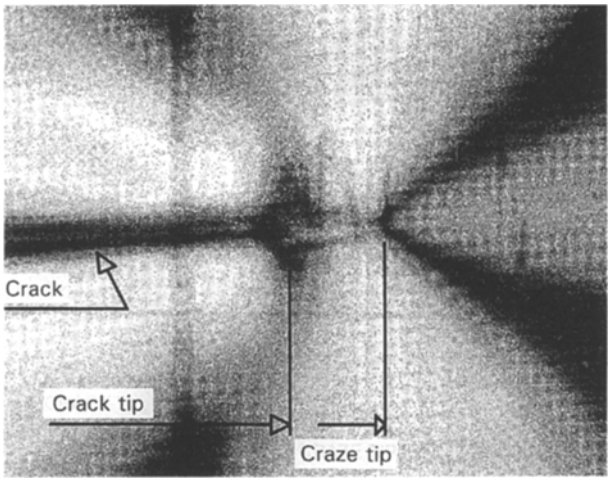


*Figure 5* Crack tip between polarizers showing the plastic-zone tip.

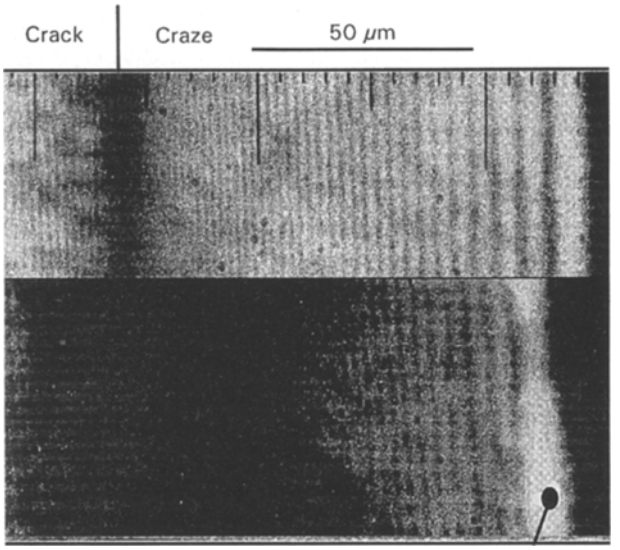


*Figure 7* Top (normal fringe pattern in water; bottom, fringe pattern at critical velocity. Air bubble (dry craze tip).

light between two crossed polarizers to visualize the birefringence due to the stress fields. The samples were immersed in water by means of a small transparent tank fitted to the grips. Fig. 4 shows the experimental apparatus. The samples were pre-cracked with a milled saw cut, and subsequently the crack was sharpened (in air) by fatigue loading at 100 Hz.

Fig. 5 shows, by means of birefringence, the crack and craze tips. Both tips can be separated and individually followed during the process if the craze (or plastic zone) is long enough to be resolved by the optical telescope.

## 3.2. Optical interferometry

The principle of optical interferometry applied to craze-profile visualization has been described elsewhere [14]. The technique allows the measurement in real-time of the craze shape and size at the running crack tip. The advantages of the method are that the craze can be very short (a few micrometres), its velocity can be high (up to 0.5 mm $s^{-1}$), and the measurement is made on a single craze at the crack tip (easy crack-tip micromechanics). The sample in the interferometer is immersed in water, and loaded in the usual way. Crack-tip interference patterns are recorded during loading, craze growth and crack–craze propagation. Each measurement gives access to the following results: crack tip and craze-tip velocities, applied load, $K_1$ and craze shape as a function of velocity. Fig. 6 shows the experimental principle, and Fig. 7 two typical fringe patterns.

The fringe patterns show that the plastic zone at the crack tip is still a craze (and not a shear zone). Moreover, the interference optical contrast shows whether or not the craze is filled with water. Clearly, below some particular value of the crack–craze velocity, the craze is wet, and above it the craze is dry. The $K_1$ values in water are identical to those measured on the tensile machine reported above. The craze shapes recorded are similar to those in air, but the craze length varies considerably with rate, as reported below. The velocity range covered by this technique is larger than that covered with the tensile machine. The importance of the interferometric fringe pattern results will be revealed below where craze micro-mechanics will be applied to measured craze shapes.

## 3.3. Results

### 3.3.1. $K_1$ versus velocity

Standardized fracture toughness measurements do not require the monitoring of the crack speed or length in a real-time experiment. Nevertheless, the results of such simplified measurements are rather scattered, one of the major reasons being the unknown crack-tip starting point on the load–deflection curve. Moreover, it is well known that the fracture toughness depends strongly on the crack velocity, which may vary over several decades at the propagation starting point. More accurate results are obtained when considering the fracture energy as a function of crack speed for brittle materials, or as a function of crack length for ductile materials. In the case of brittle materials, such as PMMA, the crack-tip velocity must be kept constant until quasi-stationary propagation is reached. The $K_1$ or $G_1$ value obtained for the particular velocity is then an intrinsic material property.

Fig. 8 shows the values of $K_1$ versus velocity for a crack tip propagating in air compared to that propagating in water. The toughness in water is about twice that in air, especially at low propagation speed. It appears that the scatter in water is much larger than that in air. Careful examination of the experimental procedure showed that the loading history (i.e. loading rate) strongly influences the $K_1$ value obtained as a function of crack speed. This is in contradiction with the behaviour in air.

### 3.3.2. $K_1$ versus loading rate

Fig. 9 shows the toughness as a function of crack speed, but with a controlled loading rate. Surprisingly, a one decade change in loading rate doubles the toughness in the 0.001 mm $s^{-1}$ velocity range. Consequently, the $K_1$ versus velocity is no longer an intrinsic material property. There exists a knee in the $K_1$ curve, which corresponds to the velocity above which the crack tip propagates steadily without increasing the plastic-zone size at its tip.

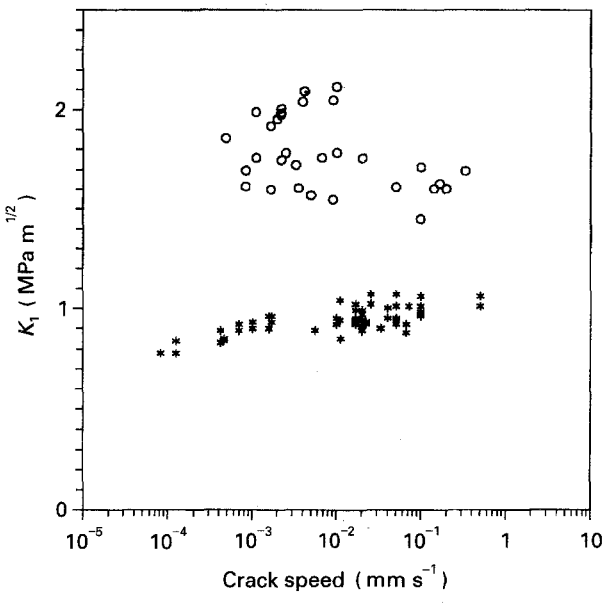


*Figure 8* Toughness versus crack velocity in (*) air, and (○) water, at 20 °C.

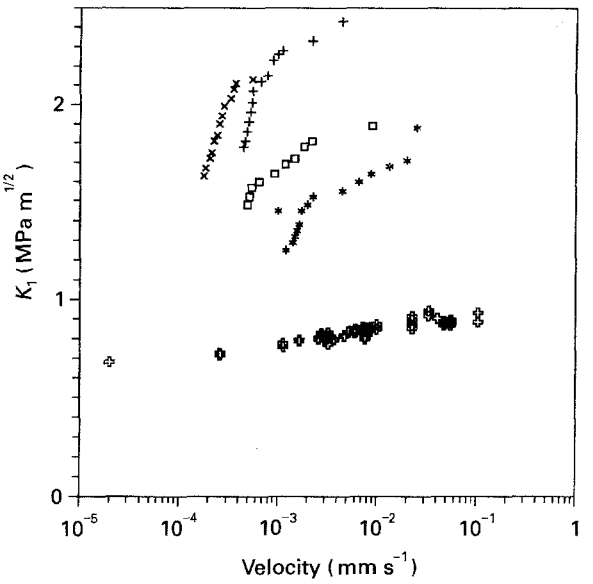


*Figure 9* Toughness versus velocity and loading rate: (*) 0.110 N $s^{-1}$, (□) 0.056 N $s^{-1}$, (+) 0.030 N $s^{-1}$, (×) 0.012 N $s^{-1}$ all in water; (⌖) any rate in air.

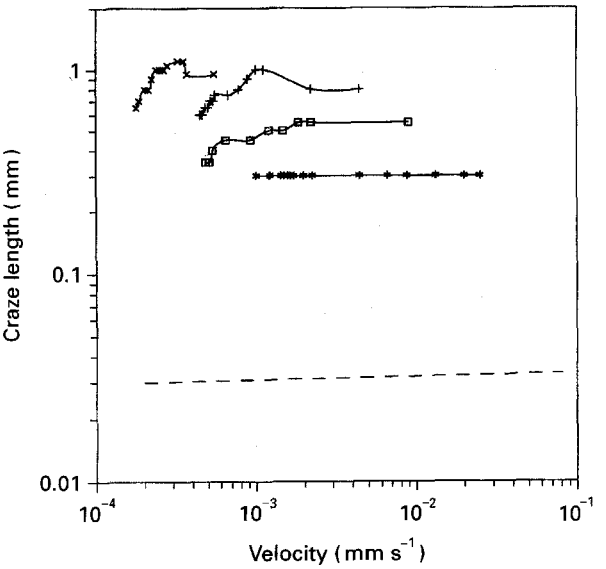


*Figure 10* Craze length versus loading rate: (*) 0.110 N $s^{-1}$, (□) 0.056 N $s^{-1}$, (+) 0.030 N $s^{-1}$, (×) 0.012 N $s^{-1}$ all in water; (---) any rate in air.

### 3.3.3. Plastic-zone size versus loading rate

The toughness varying with loading rate indicates that the plastic zone at the crack tip depends also on loading rate. Fig. 10 shows the length of the plastic zone. The size increases with decreasing loading rate: at low rates, the crack tip yields and crack-tip blunting decreases the local stress intensity. Consequently, a higher external stress is needed to propagate the crack. Finally, the plastic-zone size stabilizes and the crack + plastic-zone system propagates steadily. Interferometric experiments reported showed that the plastic zone is a craze, as it is in air, where its size is loading-rate independent.

## 4. Crack-tip model, craze micromechanics

The material near the loaded crack tip is subjected to a stress field which is divergent at the tip. Because of that field, the material is damaged near the tip, and produces either a craze, or shear lips, or a complex structure of ruined material. In the case of the craze, which corresponds to PMMA in water, as shown by Fig. 7, stresses and strains in the vicinity are known. In particular, it has been shown that the stress applied to the craze fibrils is quite constant (with a small peak at the craze tip), and that its mean value, $\sigma_c$, is a function of the stress intensity factor, $K_1$, and craze length, $S$

$$\sigma_c^2 = \pi K_1^2 / 8S \tag{2}$$

Craze fibrils originate from bulk polymer by a cavitation mechanism at the craze tip, and subsequently they grow mainly by extracting fresh material from the bulk. To some extent, they also grow by an elongation mechanism. As they are subjected to a stress, they break after a while. Each fibril is subjected to the stress during the time it takes for the craze to move over one craze length [14]. For stationary propagation, this time, $\tau_c$, which depends on the stress, $\sigma_c$, is a function of the crack–craze velocity, $v_c$

$$\tau_c(\sigma)_c = S/v_c \tag{3}$$

and hence

$$K_1(v_c) = (8\tau_c v_c/\pi)\sigma_c^{1/2} \tag{4}$$

Craze length, propagation velocity, and $K_1$ values are recorded during the experiments. Hence, the local, intrinsic material properties governing fibril extraction at the craze tip, $\sigma_c$, and that governing fibrils rupture, $\tau_c(\sigma_c)$ can be inferred.

### 4.1. Propagating crack–craze

Fig. 11 shows the craze fibril lifetime as a function of the stress applied to the fibrils. It appears that the loading rate is no longer a relevant parameter, as it was in the $K_1$ or $S$ plot. This proves that the fibril lifetime is an intrinsic material property, because it is geometry independent. The influence of the loading rate on $K_1$ and $S$ values is due to the fact that during the measurement, macroscopic stationary fracture conditions are not reached. Therefore, the transient conditions under which $K_1$ and $S$ were measured are variable and unknown. Locally, at the fibrils level, even under these macroscopic transient conditions, real intrinsic material properties govern the rupture. The plot also shows that the fibril lifetime in water is three orders of magnitude lower than that in air at a given stress on the fibrils.

Fig. 12 shows the craze-tip velocity as a function of the stress on the fibrils. This is the second relevant intrinsic material property, governing the cavitation of the bulk polymer leading to fibrils. Again, the loading rate is no longer a relevant parameter, for the same reasons. The velocity in water is also about three orders of magnitude faster than in air, and the tensile machine measurements overlap very well the interference measurements. There is an interesting zone at $10^{-1}$ mm s$^{-1}$, where the values in water rejoin those in air. This corresponds to the velocity above which water cannot flow fast enough around the fibrils to reach the craze tip, or diffuse fast enough into the fibrils to soften them. It corresponds to the picture shown in Fig. 7 where a craze tip appears dry, even though the specimen is immersed in water.

Fig. 13 shows, in detail, the transition zone, with both craze-tip and crack-tip velocities as a function of stress. For each value of stress, both velocities were measured. At low velocity, in water, the crack propagates about ten times slower than the craze ! Near the transition velocity, both crack and craze propagate at the same velocity, in a steady-state manner. This explains clearly the complicated behaviour of $K_1$ versus velocity in water: $K_1$ depends on craze length, $S$ (equation 4) which, in turn, depends on both craze and crack speed, which are not the same: there is no steady-state crack–craze propagation at low velocity

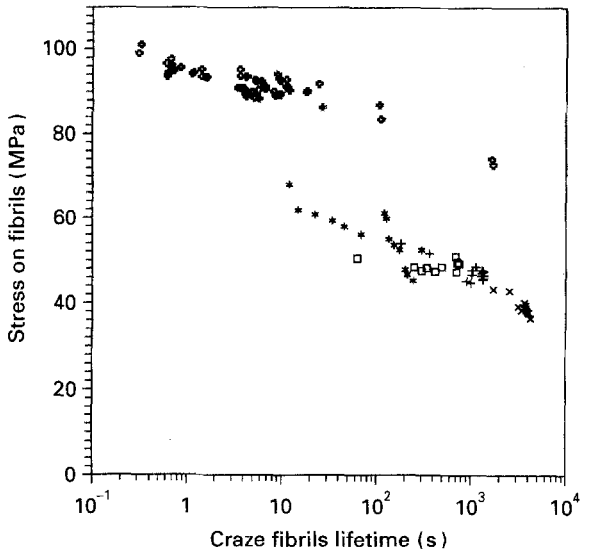


*Figure 11* Fibril lifetime (all loading rates).: For key, see Fig. 9.

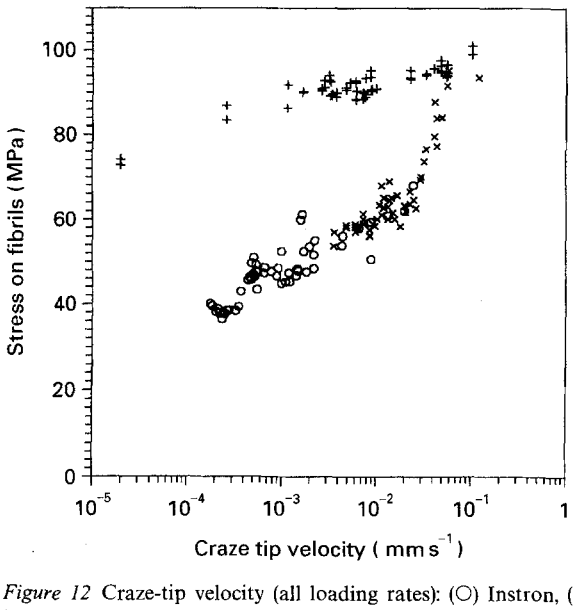


*Figure 12* Craze-tip velocity (all loading rates): (O) Instron, ( + ) interferometer (air) ( × ) interferometer (water).

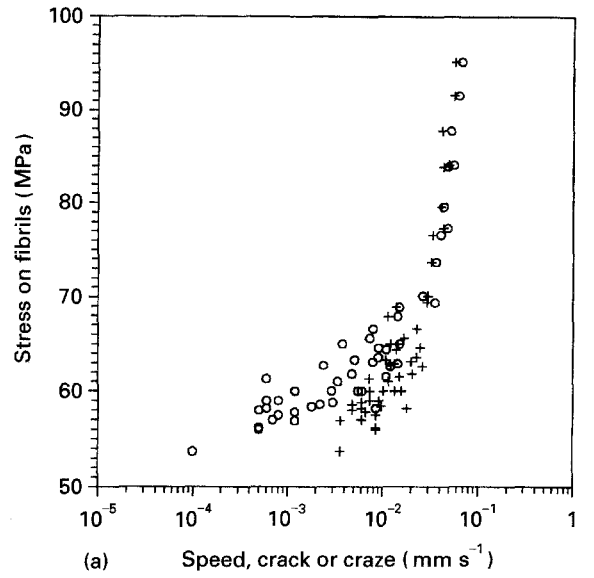


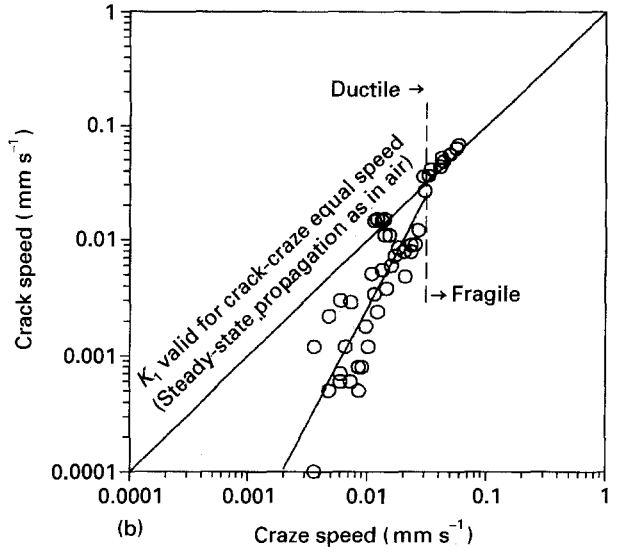


*Figure 13* Craze- and ( + ) crack-tip velocity versus craze stress for specimens in water.

## 4.2. Crack arrest and craze growth

When the sample is loaded just below the critical value leading to propagation, the crack is arrested, whereas the craze tip slowly moves, increasing the craze length. This is simply due to the fact that craze stress is time-dependent, like yield stress, and Equation 2 shows that if $\sigma_c$ decreases, $S$ increases under constant $K_1$. Fig. 14 shows the craze length versus time in that case, and Fig. 15 the inferred mean craze stress. As in air, the rate of the craze-stress decrease in water is independent of $K_1$, and the slope versus time (the relaxation process) is similar, but twice as large as that in air. Hence, the relaxation process under constant strain (the craze fibril extension ratio) if favoured by the water on the craze boundary.

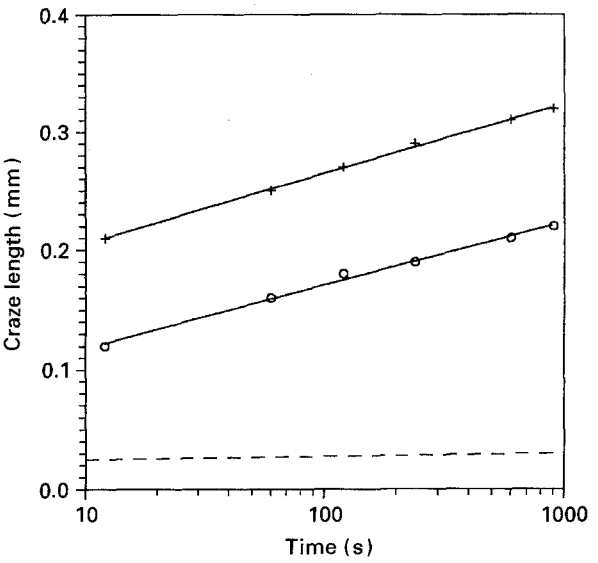


*Figure 14* Craze length versus time for $K_1$ = (O) 1.06 MPa $m^{1/2}$ (water), ( + ) 1.35 MPa $m^{1/2}$ (water) and (---) 0.6 MPa $m^{1/2}$ (air).

in water. Hence, $K_1$ cannot be uniquely defined as a function of velocity.

In summary, there are three velocity (or time) zones where different mechanisms control the crack–craze growth. Fig. 12 shows that at low velocity water plasticizes fibrils and flows quasi-instantaneously to the craze tip. The rupture is controlled by external load and crack-tip micromechanics as in air, but the stresses involved are lower. On the other hand, at high velocity, water does not plasticize the fibrils, nor flow to the craze tip, and fracture arises like in air. In the intermediate range of velocity, water-diffusion processes in the fibrils and/or water-flow mechanisms are dominant and control the crack–craze propagation velocity. Fig. 13 shows the relation between craze and crack speed as a function of the local stress on the craze fibrils. Clearly, there is a region below 0.03 mm $s^{-1}$ where the craze grows faster than the crack. Consequently, the craze length increases steadily, leading to ductile crack-tip behaviour.

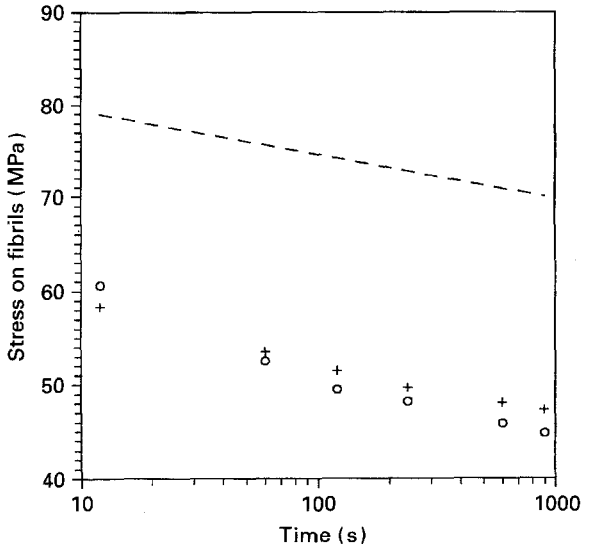


*Figure 15* Craze stress relaxation, for $K_1$ = (O) 1.06 MPa $m^{1/2}$ (water), ( + ) 1.35 MPa $m^{1/2}$ (water), and (---) any value in air.

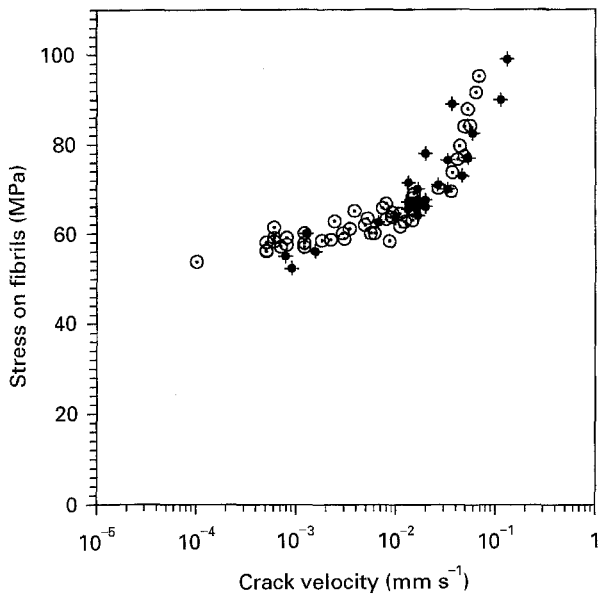


*Figure 16* Results in salt water: (⊙) pure water, (✦) salt water.

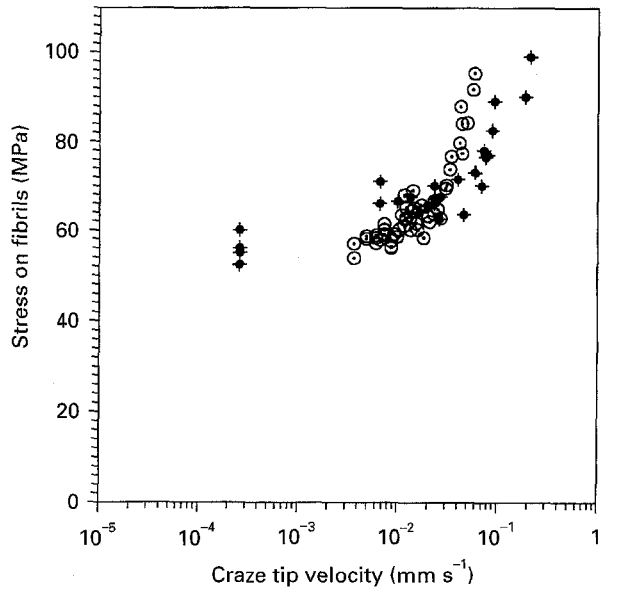


*Figure 17* Results in salt water: for key, see Fig. 16.

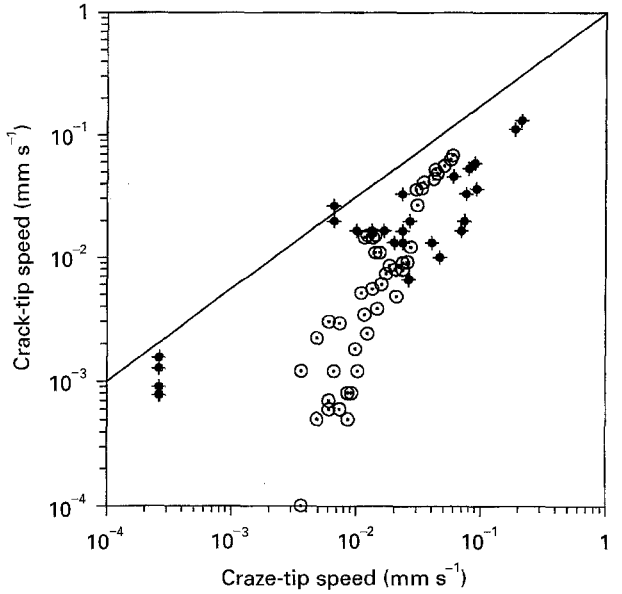


*Figure 18* Results in salt water: for key, see Fig. 16.

### 4.3. Pure water and salt water

As in real submarine applications, the surrounding water is mainly salt water, experiments were performed, in a saturated solution of water and sodium chloride salt. The results are shown in Fig. 16–18. Crack velocity (fibril breakage) is unchanged. Craze-tip velocity (fibril growth) is perhaps a little changed, but fracture toughness remains the same, insofar as $K_1(v_c)$ can be defined.

## 5. Interpretation in terms of a stress-activated process

### 5.1. Activation volume

It has been shown earlier that both fibril extraction and fibril rupture are similar to plastic flow mechanisms, and are stress- and temperature-activated processes [15]. In fact, both lifetime and craze-growth velocity are linear on log plots versus time, at least over a certain time range

$$\tau_c = \tau_0 \exp(-\sigma/\sigma_t) \tag{5}$$

and

$$v_c = v_0 \exp(+\sigma/\sigma_v) \tag{6}$$

where

$$1/\sigma_t = V_t^*/kT$$

and

$$1/\sigma_v = V_v^*/kT \tag{7}$$

Both $V_t^*$ and $V_v^*$ are apparent activation volumes, $T$ the temperature (K), and $k$ the Boltzmann's constant. The activation volumes measured on the experimental plots are, respectively, $300 \times 10^{-3}$ and $500 \times 10^{-3}$ nm$^3$ for fibril extraction and lifetime (below $10^{-2}$ mm s$^{-1}$ velocity). In air, both volumes are identical and equal to about $2100 \times 10^{-3}$ nm$^3$ and in low-pressure toluene gas (1.14 hPa) they are $330 \times 10^{-3}$ and $400 \times 10^{-3}$ nm$^3$ [15]. The physical meaning of activation volumes is rather controversial. Nevertheless, the plasticizing effect of water reduces the average size of the molecular volumes involved in the fibril drawing and breakage mechanisms. The fact that extraction and breakage activation volumes are not identical in water (as they are in air), explains the steadily increasing craze size, below the critical velocity: the fibril extraction is "easier" than their breakage, leading to steadily increasing length.

### 5.2. Diffusion coefficient

When the craze growth is diffusion controlled, it has been shown that there is a simple relationship between the craze surface velocity and the diffusion coefficient [15]. In the case of Fickian diffusion, the craze surface velocity yields

$$v_e = (D/R_0)\ln[C_0/C(S)] \tag{8}$$

where $D$ is the diffusion coefficient (cm$^2$ s$^{-1}$), $R_0$ is the fibril radius, $C_0$ the equilibrium concentration of the

liquid at the surface, $C(S)$ the concentration at the craze boundary, and $C(S)/C_0 = 0.5$. Then

$$v_e = 3 \times 10^5 D \quad (9)$$

In water, the limiting craze velocity for a liquid-controlled craze growth is about $6 \times 10^{-3}$ cm s$^{-1}$, and hence the limiting craze surface growth, $v_e$, is about $6 \times 10^{-4}$ cm s$^{-1}$ [15]. Then the diffusion coefficient yields $D = 20 \times 10^{-10}$ cm$^2$ s$^{-1}$. This value should be compared with the water-diffusion coefficient in the bulk polymer, of $1.7 \times 10^{-10}$ cm$^2$ s$^{-1}$. It is about ten times larger. This discrepancy may be explained by at least two reasons: firstly, in Equation 8 the fibril radius, $R_0$, was estimated without knowing the real value, and secondly, in highly stressed and oriented material like fibrils, with extremely high surface-to-volume ratio, the water diffusion may be faster than in bulk polymer, leading to higher diffusion coefficients. On the other hand, there is another limiting mechanism competing with diffusion, namely the water flow around the fibrils from the crack tip to the craze tip, combined with surface-tension effects between water and the polymer surface. Owing to the water viscosity, the flow reaches some limiting velocity, above which the craze remains dry, as shown in Fig. 7.

## 6. Conclusions

Water has only a slight influence on small-strain mechanical properties of PMMA, whereas fracture properties are drastically changed when the crack propagates immersed in water: the toughness increases strongly, and a linear elastic fracture mechanics approach is no longer valid. The plastic zone at the crack tip is still a craze, but its length increases steadily, leading to increasing toughness values. The water reaches the craze tip at low propagation velocity, and does not at high velocity.

There are three velocity (or time) zones where different mechanisms control the crack–craze growth: at low velocity water plasticizes fibrils and flows quasi-instantaneously to the craze tip. The rupture is controlled by external load and crack-tip micromechanics as in air, but the stresses involved are lower. Like in air, fibril-growth activation volumes and energies in water may be inferred from experiment. On the other hand, at high velocity, water does not plasticize the fibrils at all, nor does it flow to the craze tip, and fracture occurs as in air. In the intermediate range of velocity, water-diffusion processes in the fibrils and/or water-flow mechanisms are dominant and control the crack–craze propagation velocity. Salt water and pure water seem to have the same influence on the toughness of a propagating crack tip.

## References


1. J. J. BENBOW, *Proc. Phys. Soc. B* **78** (1961) 970.
2. Y. M. MAI, *J. Mater. Sci.* **10** (1975) 943.
3. V. A. KEFALAS and A. S. ARGON, *ibid.* **23** (1988) 253.
4. R. G. HILL, J. F. BATES, T. T. LEWIS and N. REES, *ibid.* **19** (1984) 1904.
5. J. G. WILLIAMS, *Adv. Polym. Sci.* **27** (1978) 67.
6. J. SHEN, C. C. CHEN and J. A. SAVER, Polymer **26** (1985) 511.
7. J. J. JANACEK and J. J. KOLARIK, *J. Polym. Sci. C* **16** (1967) 279.
8. D. T. TURNER, *Polymer* **23** (1982) 197.
9. Z. MIYAGI and K. TANAKA, *ibid.* **16** (1975) 441.
10. J. M. BARTON, *ibid.* **20** (1979) 1018.
11. P. J. BURCHILL and R. H. STACEWICZ, *J. Mater. Sci. Lett.* **1** (1982) 446.
12. D. PUTZ and G. MENGES, *Br. Polym. J.* **10** (1978) 69.
13. L. S. SMITH and J. A. SAUER, *Plast. Rubber Process.* **6** (1986) 57.
14. P. TRASSAERT and R. SCHIRRER, *J. Mater. Sci.* **18** (1983) 3004.
15. R. SCHIRRER and G. GALLERON, *Polymer* **29** (1988) 634.



*Received 7 January*
*and accepted 5 September 1994*